Heat Mass Transfer
DOI 10.1007/s00231-013-1163-6

ORIGINAL

Enhance of heat transfer on unsteady Hiemenz flow of nanofluid over a porous wedge with heat source/sink due to solar energy radiation with variable stream condition

Radiah Bte Mohamad · R. Kandasamy · I. Muhaimin

Received: 25 September 2012 / Accepted: 22 April 2013

Abstract Nanofluid-based direct solar receivers, where nanoparticles in a liquid medium can scatter and absorb solar radiation, have recently received interest to efficiently distribute and store the thermal energy. The objective of the present work is to investigate theoretically the unsteady homogeneous Hiemenz flow of an incompressible viscous nanofluid past a porous wedge due to solar energy (incident radiation). The conclusion is drawn that the temperature is significantly influenced by magnetic strength, nanoparticle volume fraction, convective radiation and porosity of the wedge sheet.

1 Introduction

Energy plays an important role in the development of human society. However, over the past century, the fast development of human society leads to the shortage of global energy and the serious environmental pollution. All countries of the world have to explore new energy sources and develop new energy technologies to find the rode to sustainable development. Solar energy as the renewable and environmental friendly energy, it has produced energy for billions of years. Solar energy that reaches the earth is around $4 \times 1{,}015$ MW, it is 2,000 times as large as the global energy consumption. Thus the utilization of solar energy and the technologies of solar energy materials attract much more attention. Nano-materials as a new energy material, since its particle size is the same as or smaller than the wavelength of de Broglie wave and coherent wave. Therefore, nanoparticle becomes to strongly absorb and selectively absorb incident radiation. Based on the radiation and Brownian motion properties of nanoparticle, the utilization of nanofluids in solar thermal system becomes the new study hotspot.

Solar energy is one of the best sources of renewable energy with minimal environmental impact, Sharma et al. [1]. Power tower solar collectors could benefit from the potential efficiency improvements that arise from using a nanofluid as a working fluid. The basic concept of using particles to collect solar energy was studied in the 1970s by Hunt [2]. It has been shown that mixing nanoparticles in a liquid (nanofluid) has a dramatic effect on the liquid thermophysical properties such as thermal conductivity. Numerous models and group theory methods have been proposed by different authors to study convective flows of nanofluids, e.g. Birkoff [3], Yurusoy and Pakdemirli [4] and Yurusoy et al. [5]. The study of the stagnation flow problem was initiated by Hiemenz [6] who developed an exact solution for the Navier-Stokes equations under a forced convective regime. Detailed review studies on Hiemenz flow are published by Chamkha and Abdul-Rahim [7], Seddeek et al. [8], Tsai and Huang [9], and Gamal and Abdel-Rahman [10] and Yih [11]. The effects of heat and mass transfer laminar boundary layer flow over a wedge have been studied by many authors in different situations.

Nanofluids are suspensions of nanoparticles in fluids that show significant enhancement of their properties at modest nanoparticle concentration was investigated by Kandasamy et al. [12], Vajravelu et al. [13] and Rana and Bhargava [14]. Solar energy is currently one kind of important resource for clean and renewable energy, and is widely investigated in many fields. Recently, non-homogeneous equilibrium model proposed by many authors, whereas several numerical studies on homogeneous modeling of natural convection heat transfer in nanofluids have been published by Ahmad

R. B. Mohamad · R. Kandasamy (✉) · I. Muhaimin
Research Centre for Computational Mathematics, FSTPI,
Universiti Tun Hussein Onn Malaysia, Batu Pahat, Malaysia
e-mail: future990@gmail.com; ramasamy@uthm.edu.my

Journal : Large 231 | Dispatch : 29-4-2013 | Pages : 9
Article No. : 1163 | LE | TYPESET
MS Code : HMT-12-0378 | CP | DISK

et al. [15], Yacob et al. [16], Hamad [17] and Magyari [18] because the dispersed and the continuous phases are combined together and modeled as a new continuous phases in which the velocity slip between the phases must be small. The homogeneous flow model provides the simplest technique for analyzing multiphase flows.

The aim of the present study is to investigate the development of the unsteady homogeneous Hiemenz boundary layer flow and heat transfer over a porous wedge sheet in a nanofluid due to solar radiation. Lie symmetry group transformation is utilized to convert the governing partial differential equations into ordinary differential equations and then the numerical solution of the problem is accomplished by using Runge-Kutta Gill method [19] with shooting technique. This method has the following advantages over other available methods: (1) it utilizes less storage register (2) it controls the growth of rounding errors and is usually stable and (3) it is computationally economical. Numerical calculations were carried out for different values of dimensionless parameters of the problem under consideration for the purpose of illustrating the results graphically. The analysis of the results obtained shows that the flow field is influenced appreciably by the presence of convective radiation and nanoparticles deposition in the presence of nanofluid past a porous wedge sheet.

2 Mathematical analysis

Consider the unsteady laminar two- dimensional Hiemenz flow of an incompressible viscous nanofluid past a porous wedge sheet in the presence of solar energy radiation (see, Fig. 1). We consider influence of a constant magnetic field of strength B_0 which is applied normally to the sheet. The temperature at the wedge surface takes the constant value T_w, while the ambient value, attained as y tends to infinity, takes the constant value T_∞. Far away from the wedge plate, both the surroundings and the Newtonian, absorbing fluid are maintained at a constant temperature T_∞. It is further assumed that the induced magnetic field is negligible in comparison to the applied magnetic field (as the magnetic Reynolds number is small). The porous medium is assumed to be transparent and in thermal equilibrium with the fluid. The thermal dispersion effect is minimal when the thermal diffusivity of the porous matrix is of the same order of magnitude as that of the working fluid. This viewpoint of assuming that the effective thermal diffusivity remains constant when the porosity of the porous medium varies with the normal distance is shared by many other investigators such as Vafai et al. [20] and Tien and Hong [21]. The non reflecting absorbing ideally transparent wedge plate receives an incident radiation flux of intensity q''_{rad}. This radiation flux penetrates the plate and is absorbed in an adjacent fluid of absorption coefficient, Fathalah and Elsayed [22]. Due to heating of the absorbing nanofluid and the wedge plate by solar radiation. heat is transferred from the plate to the surroundings and the solar radiation is a collimated beam that is normal to the plate. The fluid is a water based nanofluid containing copper nanoparticles. As mentioned before, the working fluid is assumed to have heat absorption properties. For the present application, the porous medium absorbs the incident solar radiation and transits it to the working fluid by convection. The thermophysical properties of the nanofluid are given in Table 1 (see Oztop and Abu-Nada [23]. Under the above assumptions, the boundary layer equations governing the flow and thermal field can be written in dimensional form as

$$\frac{\partial \bar{u}}{\partial \bar{x}} + \frac{\partial \bar{v}}{\partial \bar{y}} = 0 \tag{1}$$

$$\frac{\partial \bar{u}}{\partial \bar{t}} + \bar{u}\frac{\partial \bar{u}}{\partial \bar{x}} + \bar{v}\frac{\partial \bar{u}}{\partial \bar{y}} = \frac{1}{\rho_{f_n}}\left[\left(\frac{\partial U}{\partial t} + U\frac{dU}{dx}\right)\rho_{f_n} + \mu_{f_n}\frac{\partial^2 \bar{u}}{\partial \bar{y}^2} + (\rho\beta)_{f_n}\bar{g}(T - T_\infty)\cos\frac{\Omega}{2} - \left(\sigma B_0^2 + \frac{\nu_{f_n}}{K}\rho_{f_n}\right)(\bar{u} - U)\right] \tag{2}$$

$$\frac{\partial T}{\partial \bar{t}} + \bar{u}\frac{\partial T}{\partial \bar{x}} + \bar{v}\frac{\partial T}{\partial \bar{y}} = \alpha_{f_n}\frac{\partial^2 T}{\partial \bar{y}^2} - \frac{1}{(\rho c_p)_{f_n}}\frac{\partial q''_{rad}}{\partial y} - \frac{Q_0}{(\rho c_p)_{f_n}}(T - T_\infty) \tag{3}$$

Using Rosseland approximation for radiation (Sparrow and Cess [24], Rapits [25] and Brewster [26]) we can write $q''_{rad} = -\frac{4\sigma_1}{3k^*}\frac{\partial T^4}{\partial y}$ where σ_1 is the Stefan–Boltzman constant is, k^* is the mean absorption coefficient. The Rosseland approximation is used to describe the radiative heat transfer in the limit of the optically thick fluid (nanofluid). The term $Q_0(T_\infty - T)$ is assumed to be the amount of heat generated/absorbed per unit volume. Q_0 is a constant, which may

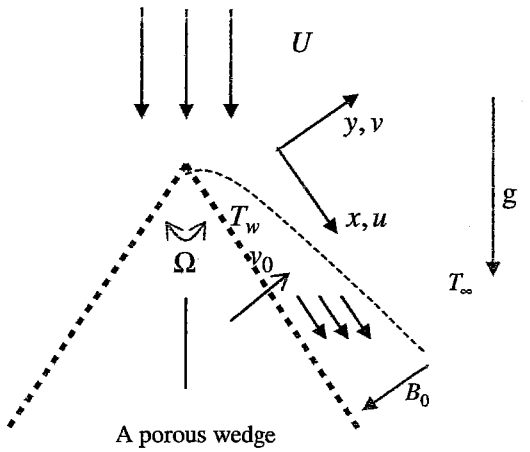

Fig. 1 Physical flow model over a porous wedge sheet

Journal : Large 231 | Dispatch : 29-4-2013 | Pages : 9
Article No. : 1163 | LE | TYPESET
MS Code : HMT-12-0378 | CP | DISK

take on either positive or negative values. When the wall temperature T_w exceeds the free stream temperature T_∞, the source term represents the heat source when $Q_0 < 0$ and heat sink when $Q_0 > 0$.

The boundary conditions of these equations are

$$\bar{u} = 0, \bar{v} = -v_0, \quad T = T_w + c_1 x^{n_1} \text{ at } \bar{y} = 0;$$
$$\bar{u} \longrightarrow U = \frac{v_f x^m}{\delta^{m+1}}, \quad T \to T_\infty \text{ as } \bar{y} \to \infty \tag{4}$$

where c_1 and n_1 (power index) are constants and V_0 and T_w are the suction (>0) or injection (<0) velocity and the fluid temperature at the plate. Under this consideration, the potential flow velocity of the wedge can be written as $U(x,t) = \frac{v_f x^m}{\delta^{m+1}}$, $\beta_1 = \frac{2m}{1+m}$ (see in Sattar [27]) whereas δ is the time-dependent length scale which is taken to be (detailed in Sattar [27]) as: $\delta = \delta(t)$ and β_1 is the Hartree pressure gradient parameter that corresponds to $\beta_1 = \frac{\Omega}{\pi}$ for a total angle Ω of the wedge, the temperature of the fluid is assumed to vary following a power-law function while the free stream temperature is linearly stratified. The suffixes w and ∞ denote surface and ambient conditions. Here $\bar{u}$ and $\bar{v}$ are the velocity components in the $\bar{x}$ and $\bar{y}$ directions, T is the local temperature of the nanofluid, $\bar{g}$ is the acceleration due to gravity, V_o is the velocity of suction/injection, K is the permeability of the porous medium, ρ_{f_n} is the effective density of the nanofluid, q''_{rad} is the applied absorption radiation heat transfer, μ_{f_n} is the effective dynamic viscosity of the nanofluid, α_{f_n} is the thermal diffusivity of the nanofluid which are defined as (see Aminossadati and Ghasemi [28]),

$$\rho_{f_n} = (1-\zeta)\rho_f + \zeta\rho_s, \quad \mu_{f_n} = \frac{\mu_f}{(1-\zeta)^{2.5}}$$

$$(\rho\beta)_{f_n} = (1-\zeta)(\rho\beta)_f + \zeta(\rho\beta)_s, \quad \alpha_{f_n} = \frac{k_{f_n}}{(\rho c_p)_{f_n}},$$

Maxwell model [29] was developed to determine the effective electrical or thermal conductivity of liquid–solid suspensions. This model is applicable to statistically homogeneous and low volume concentration liquid–solid suspensions, with randomly dispersed and uniformly sized non-contacting spherical particles. It is given as:

$$\frac{k_{f_n}}{k_f} = \left\{\frac{(k_s + 2k_f) - 2\zeta(k_s - k_f)}{(k_s + 2k_f) + 2\zeta(k_s - k_f)}\right\} \tag{5}$$

Experiments report thermal conductivity enhancement of nanofluids be yond the Maxwell limit of 3ζ. In the limit of low particle volume concentration (ζ) and the particle conductivity (k_s), being much higher than the base liquid conductivity (k_f), Eq. (5) can be reduced to Maxwell 3ζ limit as:

$$k_{low} = \frac{k_{f_n}}{k_f} = 1 + 3\zeta \tag{6}$$

Equation (5) represents the lower limit for the thermal conductivity of nanofluids and it can seen that in the limit where $\zeta = 0$ (no particles), Eq. (6) yields $k_{low} = 1$ as expected.

Where k_f and k_s are the thermal conductivity of the base fluid and nanoparticle respectively, ζ is the nanoparticle volume fraction, μ_f is the dynamic viscosity of the base fluid, β_f and β_s are the thermal expansion coefficients of the base fluid and nanoparticle, respectively, ρ_f and ρ_s are the density of the base fluid and nanoparticle, respectively, k_{f_n} is the effective thermal conductivity of the nanofluid and $(\rho c_p)_{f_n}$ is the heat capacitance of the nanofluid, which are defined as

$$(\rho c_p)_{f_n} = (1-\zeta)(\rho c_p)_f + \zeta(\rho c_p)_s$$

Equations (1–4) take the non-dimensional form

$$\frac{\partial u}{\partial x} + \frac{\partial v}{\partial y} = 0 \tag{7}$$

$$\frac{\partial u}{\partial t} + u\frac{\partial u}{\partial x} + v\frac{\partial u}{\partial y} = \frac{1}{\left(1-\zeta+\zeta\frac{\rho_s}{\rho_f}\right)}\left\{\left(1-\zeta+\zeta\frac{(\rho\beta)_s}{(\rho\beta)_f}\right)\gamma\sin\frac{\Omega}{2}\theta\right\} + \frac{1}{\left(1-\zeta+\zeta\frac{\rho_s}{\rho_f}\right)}\left[\left(\frac{\partial U}{\partial t} + U\frac{dU}{dx}\right)\frac{\rho_{f_n}}{\rho_f} + \frac{1}{(1-\zeta)^{2.5}}\frac{\partial^2 u}{2} - \left(\frac{\sigma B_0^2}{\rho_f} + \frac{\mu_{f_n}}{\rho_f K}\right)(u-U)\right] \tag{8}$$

Table 1 Comparison of the current results with previous published work

η	White [32]			Present works		
	$f(\eta)$	$f'(\eta)$	$f''(\eta)$	$f(\eta)$	$f'(\eta)$	$f''(\eta)$
0.0	0.000000	0.000000	0.469599	0.000000	0.000000	0.469686
0.5	0.05864	0.23423	0.46503	0.058656	0.234267	0.465078
1.0	0.23299	0.46063	0.43438	0.232986	0.460628	0.434377
2.0	0.88680	0.81669	0.25567	0.886797	0.816687	0.255668
3.0	1.79557	0.96905	0.06771	1.795569	0.969046	0.067714
4.0	2.78388	0.99777	0.00687	2.783882	0.997773	0.006871

Journal : Large 231 Dispatch : 29-4-2013 Pages : 9
Article No. : 1163 LE TYPESET
MS Code : HMT-12-0378 CP DISK

$$\frac{\partial\theta}{\partial t}+u\frac{\partial\theta}{\partial x}+v\frac{\partial\theta}{\partial y}=\frac{1}{1-\zeta+\zeta\frac{(\rho c_p)_s}{(\rho c_p)_f}} \times\left[\frac{1}{\mathrm{Pr}}\left\{\frac{k_{f_n}}{k_f}\frac{\partial^2\theta}{\partial y^2}+\frac{4}{3}N\left((C_T+\theta)^3\theta'\right)'\right\}-\frac{Q_0\Delta T}{(\rho c_p)_f}\theta\right] \quad (9)$$

with the boundary conditions

$$u=0, v=-v_0, \quad T=T_w \text{ at } y=0;$$
$$u\to U=\frac{v_f x^m}{\delta^{m+1}}, \quad T\to T_\infty \text{ as } y\to\infty \quad (10)$$

In the above equations, ζ denotes the volume fraction of the nanoparticles in the nanofluid. With the usual definition of the stream function, $u=\frac{\partial\psi}{\partial y}$ and $v=-\frac{\partial\psi}{\partial x}$, and with the aid of Kafoussias and Nanousis [30], the changes of variables are

$$\eta=y\sqrt{\frac{(1+m)}{2}}\sqrt{\frac{x^{m-1}}{\delta^{m+1}}}, \quad \psi=\sqrt{\frac{2}{1+m}}\frac{v_f x^{\frac{m+1}{2}}}{\delta^{\frac{m+1}{2}}}f(\eta) \quad \text{and} \quad \theta=\frac{T-T_\infty}{T_w-T_\infty}$$

Equations (8) and (9) are calculated using classical Lie group approach, Kandasamy [12] and Yurusoy and Pakdemirli [4].

The system of Eqs. (8, 9) become

$$\frac{1}{\left(1-\zeta+\zeta\frac{\rho_s}{\rho_f}\right)(1-\zeta)^{2.5}}f-\frac{2m}{m+1}\dot{f}^2+f\ddot{f}+\lambda_u(2\dot{f}+\eta\ddot{f})-\frac{1-m}{1=m}\xi\frac{\partial f}{\partial\xi}\left(\frac{\partial\dot{f}}{\partial\eta}-\frac{\partial\dot{f}}{\partial\eta}\right)+2\left\{\frac{m}{m+1}+\lambda_u\right\}(1-\zeta)^{2.5}+\xi^4\gamma\sin\frac{\Omega}{2}\theta-\xi^2\{M+\lambda\}(\dot{f}-1)=0 \quad (11)$$

$$\frac{1}{\mathrm{Pr}_f}\frac{\frac{k_{f_n}}{k_f}}{1-\zeta+\zeta\frac{(\rho c_p)_s}{(\rho c_p)_f}}\left[\ddot{\theta}+\frac{4}{3}N\left\{(C_T+\theta)^3\dot{\theta}\right\}'-\frac{2}{1+m}\xi^2\delta_1\theta\right] -\frac{2n_1}{m+1}\dot{f}\theta+f\dot{\theta}+\eta\lambda_u\dot{\theta}-\frac{1-m}{1+m}\left\{\xi\frac{\partial\theta}{\partial\xi}\frac{\partial f}{\partial\eta}-\xi\frac{\partial f}{\partial\xi}\frac{\partial\theta}{\partial\eta}\right\}=0 \quad (12)$$

The boundary conditions take the following form

$$\dot{f}=0, \quad \frac{m+1}{2}f+\frac{1-m}{2}\xi\frac{\partial f}{\partial\xi}=-S, \quad \theta=1 \text{ at } \eta=0 \text{ and } \dot{f}=1, \quad \theta\to 0 \text{ as } \eta\to\infty \quad (13)$$

where $\mathrm{Pr}=\frac{\nu_f}{\alpha_f}$ is the Prandtl number, $\lambda=\frac{\delta^{m+1}}{K k^2}$ is the porous media parameter, $\gamma=\frac{g(\rho\beta)_{f_n}\Delta T}{\rho_{f_n}U^2k^{\frac{2}{1-m}}}$ is the buoyancy or natural convection parameter, $\delta_1=\frac{Q_0\delta^{m+1}}{(\rho c_p)_{f_n}k^2}$ heat source/sink parameter, $N=\frac{4\sigma_1\theta_w^3}{k_{f_n}k^*}$ is the conductive radiation parameter, $M=\frac{\sigma B_0^2}{\mu_{f_n}}\frac{\delta^{m+1}}{k^2}$ is the magnetic parameter and $C_T=\frac{T_\infty}{T_w-T_\infty}$ is the temperature ratio where C_T assumes very small values by its definition as T_w-T_∞ is very large compared to T_∞. In the present study, it is assigned the value 0.1. It is worth mentioning that $\gamma>0$ aids the flow and $\gamma<0$ opposes the flow, while $\gamma=0$ i.e., (T_w-T_∞) represents the case of forced convection flow. On the other hand, if γ is of a significantly greater order of magnitude than one, then the buoyancy forces will be predominant. Hence, combined convective flow exists when $\gamma=O(1)$. S is the suction parameter if $S>0$ and injection if $S<0$ and $\xi=kx^{\frac{1-m}{2}}$ Kafoussias and Nanousis [30], is the dimensionless distance along the wedge ($\xi>0$). In this system of equations, it is obvious that the nonsimilarity aspects of the problem are embodied in the terms containing partial derivatives with respect to ξ. This problem does not admit similarity solutions. Thus, with ξ-derivative terms retained in the system of equations, it is necessary to employ a numerical scheme suitable for partial differential equations for the solution. Formulation of the system of equations for the local nonsimilarity model with reference to the present problem will now be discussed.

At the first level of truncation, the terms accompanied by $\xi\frac{\partial}{\partial\xi}$ are small. This is particularly true when ($\xi\ll 1$). Thus the terms with $\xi\frac{\partial}{\partial\xi}$ on the right-hand sides of Eqs. (11) and (12) are deleted to get the following system of equations:

$$f-\frac{2m}{m+1}\dot{f}^2+f\ddot{f}+\lambda_u(2\dot{f}+\eta\ddot{f}) +2\left\{\frac{m}{m+1}+\lambda_u\right\}(1-\zeta)^{2.5}+\xi^4\gamma\sin\frac{\Omega}{2}\theta -\xi^2\{M+\lambda\}(\dot{f}-1)=0 \quad (14)$$

$$\frac{1}{\mathrm{Pr}_{f_n}}\left[\ddot{\theta}+\frac{4}{3}N\left\{(C_T+\theta)^3\dot{\theta}\right\}'-\frac{2}{1+m}\xi^2\delta_1\theta\right] -\frac{2n_1}{m+1}\dot{f}\theta+f\dot{\theta}+\eta\lambda_u\dot{\theta}=0 \quad (15)$$

The boundary conditions take the following form

Journal : Large 231 | Dispatch : 29-4-2013 | Pages : 9
Article No. : 1163 | LE | TYPESET
MS Code : HMT-12-0378 | CP | DISK

$$\dot{f}=0,\quad \frac{m+1}{2}f+\frac{1-m}{2}\xi\frac{\partial f}{\partial\xi}=-S,\quad \theta=1\quad \text{at}\quad \eta=0$$
$$\text{and}\quad \dot{f}=1,\theta\to 0\quad \text{as}\quad \eta\to\infty \tag{16}$$

Further, we suppose that $\lambda_v=\frac{c}{x^{m-1}}$ where c is a constant so that $c=\frac{\delta^m}{\nu_f}\frac{d\delta}{dt}$ and integrating, it is obtained that $\delta=\left[c(m+1)\nu_f t\right]^{\frac{1}{m+1}}$. When $c=2$ and $m=1$ in δ and we get $\delta=2\sqrt{\nu_f t}$ which shows that the parameter δ can be compared with the well established scaling parameter for the unsteady boundary layer problems (see Schlichting [31]).

Based on homogeneous nanofluid flow, Magyari [18], the neglected velocity-slip effects in the energy equation with the help of scaling group transformations of the independent and dependent variables, $\eta=\sqrt{b}\xi_1$, $f(\eta)=\sqrt{b}f(\xi_1)$, where

$$b=\frac{\nu_{f_n}}{\nu_f}=\frac{1}{\left(1-\zeta+\zeta\frac{\rho_s}{\rho_f}\right)(1-\zeta)^{2.5}} \tag{17}$$

Equations (8–9) becomes

$$f'''-\frac{2m}{m+1}f'^2+ff''+\lambda_u(2f'+\eta f'')$$
$$+2\left\{\frac{m}{m+1}+\lambda_u\right\}(1-\zeta)^{2.5}+\xi^4\gamma\sin\frac{\Omega}{2}\theta$$
$$-\xi^2\{M+\lambda\}(f'-1)=0 \tag{18}$$

$$\frac{1}{\mathrm{Pr}_{f_n}}\left[\theta''+\frac{4}{3}N\left\{(C_T+\theta)^3\theta'\right\}'-\frac{2}{1+m}\xi^2\delta_1\theta\right]$$
$$-\frac{2n_1}{m+1}f'\theta+f\theta'+\eta\lambda_u\theta'=0 \tag{19}$$

$$f'=0,\quad f=-\frac{2S}{m+1},\quad \theta=1\quad \text{at}\quad \eta=0\quad \text{and}$$
$$f'=1,\quad \theta\to 0\quad \text{as}\quad \eta\to\infty \tag{20}$$

where $\mathrm{Pr}_{f_n}=\frac{\nu_{f_n}}{\alpha_{f_n}}=\frac{1-\zeta+\zeta\frac{(\rho c_p)_s}{(\rho c_p)_f}}{\left(1-\zeta+\zeta\frac{\rho_s}{\rho_f}\right)(1-\zeta)^{2.5}}\frac{k_f}{k_{f_n}}\mathrm{Pr}_f$ stands for the effective Prandtl number, $\mathrm{Pr}_{f_n}=\mathrm{Pr}_f$ if $\zeta=0,\frac{k_f}{k_{f_n}}=1$ (base fluid), the dimensionless velocity profiles $\dot{f}(\eta)=f'(\xi_1)=f'(\frac{\eta}{\sqrt{b}})$ and $f''(0)=\sqrt{b}\ddot{f}(0)$.

For practical purposes, the functions $f'(\eta)$ and $\theta(\eta)$ allow us to determine the skin friction coefficient

$$C_f=\frac{\mu_{f_n}}{\rho_f U^2}\left(\frac{\partial u}{\partial y}\right)_{\text{at } y=0}=-\frac{1}{(1-\zeta)^{2.5}}(\mathrm{Re}_x)^{-\frac{1}{2}}\frac{f''(0)}{\sqrt{b}} \tag{21}$$

and the Nusselt number

$$Nu_x=\frac{xk_{f_n}}{k_f(T_w-T_\infty)}\left(\frac{\partial T}{\partial y}\right)_{\text{at } y=0}$$
$$=-(\mathrm{Re}_x)^{\frac{1}{2}}\frac{k_{f_n}}{k_f}\frac{\theta'(0)}{\sqrt{b}}\left[1+\frac{4}{3}N(C_T+\theta(0))^3\right] \tag{22}$$

respectively. Here, $\mathrm{Re}_x=\frac{Ux}{\nu_f}$ is the local Reynolds number.

3 Results and discussion

The set of nonlinear ordinary differential Eqs. (18) and (19) with boundary conditions (20) have been solved by using the Runge–Kutta-Gill method [19] in conjunction with shooting technique with ζ, λ, n_1, λ_v, S, Ω, δ_1, M and N as prescribed parameters. The computations were done by a computer program which uses a symbolic and computational computer language MATLAB. A step size of $\Delta\eta=0.001$ was selected to be satisfactory for a convergence criterion of 10^{-6} in nearly all cases. The value of η_∞ was found to each iteration loop by assignment statement $\eta_\infty=\eta_\infty+\Delta\eta$. The maximum value of η_∞, to each group of parameters ζ, λ, n_1, S, Ω, λ_v, δ_1, M and N determined when the values of unknown boundary conditions at $\eta=0$ not change to successful loop with error less than 10^{-6}. The case $\gamma\gg 1.0$ corresponds to pure free convection, $\gamma=1.0$ corresponds to mixed convection and $\gamma\ll 1.0$ corresponds to pure forced convection. Throughout this calculation we have considered $\gamma=2.0$ unless otherwise specified. In order to validate our method, we have compared the results of $f(\eta)$, $f'(\eta)$ and $f''(\eta)$ for various values of η (Table 2) with those of White [32] and found them in excellent agreement.

In the absence of energy equation, in order to ascertain the accuracy of our numerical results, the present study is compared with the available exact solution in the literature. The velocity profiles for different values of m are compared with the available exact solution of Schlichting [31], is shown in Fig. 2. It is observed that the agreement with the theoretical solution of velocity profile for different values of m is excellent.

Figures 3 and 4 present typical profiles for temperature for different values of magnetic parameter in the case of pure water and Cu–water (nanofluid). Due to the uniform convective radiation, it is clearly shown that the above mentioned two cases, the temperature of the fluid accelerates with increase of the strength of magnetic field, which implies that the applied magnetic field tends to heat the fluid and enhances the heat transfer from the wall. As it move away from the plate, the effect of M becomes less pronounced. The effects of a transverse magnetic field to an electrically conducting fluid gives rise to a resistive-type

Journal : Large 231 | Dispatch : 29-4-2013 | Pages : 9
Article No. : 1163 | LE | TYPESET
MS Code : HMT-12-0378 | CP | DISK

Table 2 Thermophysical properties of fluid and nanoparticles

	ρ (kg m^{-3})	c_p (J kg^{-1} K^{-1})	k (W mK^{-1})	$\beta \times 10^{-5}$ (K^{-1})
Pure water ($\zeta = 0.0$)	997.1	4,179	0.613	21
Copper (Cu) ($\zeta = 0.05$)	8,933	385	401	1.67
Silver (Ag) ($\zeta = 0.1$)	10,500	235	429	1.89
Alumina (Al_2O_3) ($\zeta = 0.15$)	3,970	765	40	0.85
Titanium (TiO_2) ($\zeta = 0.2$)	4,250	686.2	8.9538	0.9

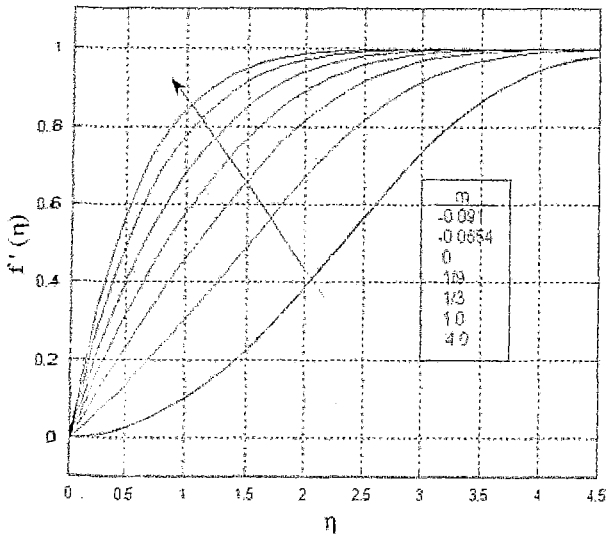

Fig. 2 Effects of m on the velocity profiles in the laminar flow past a wedge

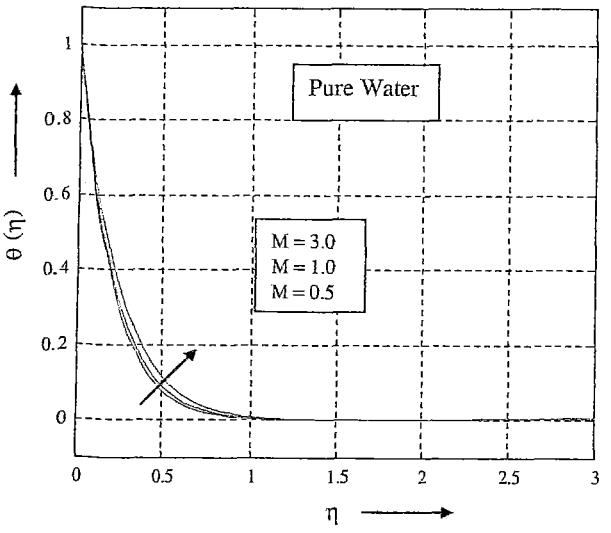

Fig. 3 Temperature profiles for various values of M–Pure water $\zeta = 0.00, \lambda_0 = 0.1, N = 0.5,\ \delta_1 = 1.0$ and $m = 0.0909\ (\Omega = 30°)$

force called the Lorentz force. This force clearly indicates that the transverse magnetic field opposes the transport phenomena and it has the tendency to slow down the motion of the fluid and to accelerate its temperature

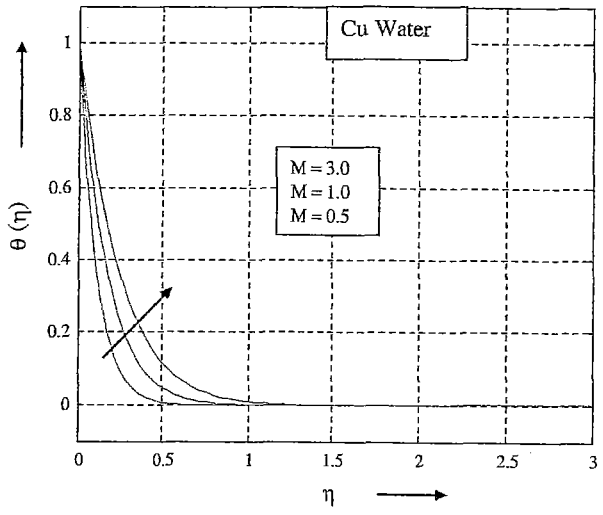

Fig. 4 Temperature profiles for various values of M $\zeta = 0.05$, $\lambda_0 = 0.1, N = 0.5,\ \delta_1 = 1.0$ and $m = 0.0909\ (\Omega = 30°)$

profiles. In all cases, the temperature vanishes at some large distance from the surface of the wedge. This result qualitatively agrees with the expectations, since magnetic field exerts retarding force on the natural convection flow. Physically, it is interesting to note that the temperature of the nanofluid (Cu Water) increases significantly as compared to that of the base fluid, because the copper Cu has high thermal conductivity. Magnetic nanofluid is a unique material that has both the liquid and magnetic properties. Many of the physical properties of these fluids can be tuned by varying magnetic field. These results clearly demonstrate that the magnetic field can be used as a means of controlling the flow and heat transfer characteristics.

Figure 5 displays the effects of volume fraction of the nanoparticles on the temperature distribution. In the presence of uniform magnetic field, it is note that the temperature of the fluid enhances with increase of the nanoparticle volume fraction parameter, ζ. The sensitivity of thermal boundary layer thickness with ζ is related to the increased thermal conductivity of the nanofluid. In fact, higher values of thermal conductivity are accompanied by higher values of thermal diffusivity. The high value of thermal diffusivity causes a drop in the temperature gradients and accordingly increases the boundary thickness as demonstrated in Fig. 5. This agrees with the physical behavior that when the

Journal : Large 231 Dispatch : 29-4-2013 Pages : 9
Article No. : 1163 LE TYPESET
MS Code : HMT-12-0378 CP DISK

volume fraction of copper raises the thermal conductivity and then the thermal boundary layer thickness increases. Changes in the size, shape, material and volume fraction of the nanoparticles allows for tuning to maximize spectral absorption of solar energy throughout the fluid volume because the nanoparticle volume fraction parameter depends on the size of the particles. Enhancement in thermal conductivity can lead to efficiency improvements, although small, via more effective fluid heat transfer. In general nanofluids show many excellent properties promising for heat transfer applications. Despite many interesting phenomena described and understood there are still several important issues that need to be solved for practical application of nanofluids.

Figures 6 and 7 present the characteristic temperature profiles for different values of the convective radiation parameter N in the presence of base fluid (pure water) and nanofluid (Cu–water). According to Eqs. (2) and (3), the divergence of the radiative heat flux increases as thermal conductivity of the fluid (k_f) falls which in turn increases the rate of radiative heat transferred to the nanofluid and hence the fluid temperature decelerates. In view of this explanation, the effect of convective radiation becomes more significant as $N \to 0$ ($N \neq 0$) and can be neglected when $N \to \infty$. It is noticed that the temperature reduces with increase of the radiation parameter N. The effect of radiation parameter N is to reduce the temperature significantly in the flow region. Further, it is noticed that the temperature of a nanofluid is decelerated significantly as compared to that of the base fluid.

The effects of unsteadiness parameter λ_v on the dimensionless temperature profiles within the nanofluid boundary-layer have been displayed in Fig. 8. It is observed that the temperature of the nanofluid increases with the increase of unsteadiness parameter λ_v. The variation of the Prandtl number within the boundary layer for different values of the unsteadiness parameter λ_v plays a dominant role on nanofluid flow field. The reason for this behavior is that the inertia of the porous medium provides an additional resistance to the fluid flow mechanism, which causes the fluid to move at a retarded rate with reduced velocity. Effect of heat source ($\delta > 0$) on temperature distribution for base fluid (pure water) and nanofluid (Cu–

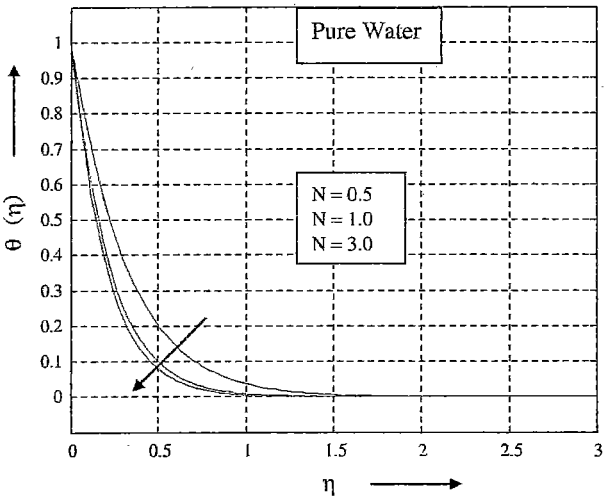

Fig. 6 Effects of convective radiation over temperature profiles $\zeta = 0.00, \lambda_v = 0.1, M = 1.0, \delta_1 = 1.0$ and $m = 0.0909$ ($\Omega = 30°$)

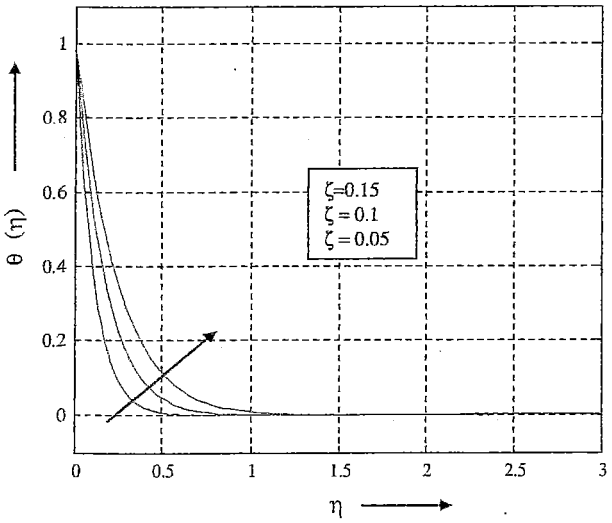

Fig. 5 Temperature profiles for various values of ζ $N = 0.5, \lambda_v = 0.1, M = 1.0, \delta_1 = 1.0$ and $m = 0.0909$ ($\Omega = 30°$)

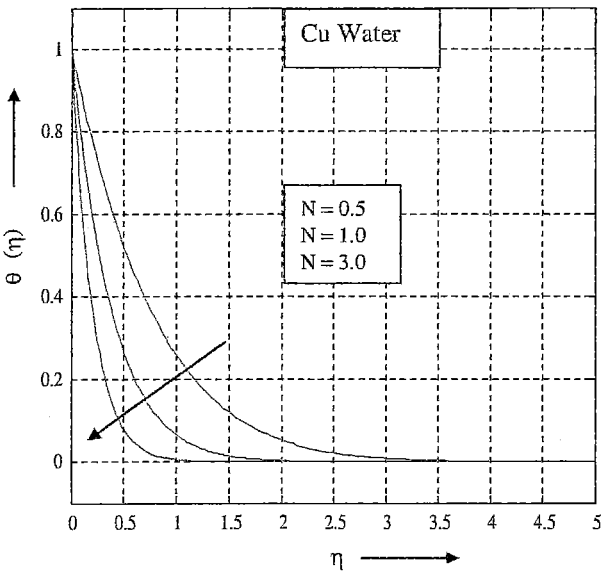

Fig. 7 Effects of convective radiation over temperature profiles $\zeta = 0.05, \lambda_v = 0.1, M = 1.0, \delta_1 = 1.0$ and $m = 0.0909$ ($\Omega = 30°$)

Journal : Large 231 | Dispatch : 29-4-2013 | Pages : 9
Article No. : 1163 | LE | TYPESET
MS Code : HMT-12-0378 | CP | DISK

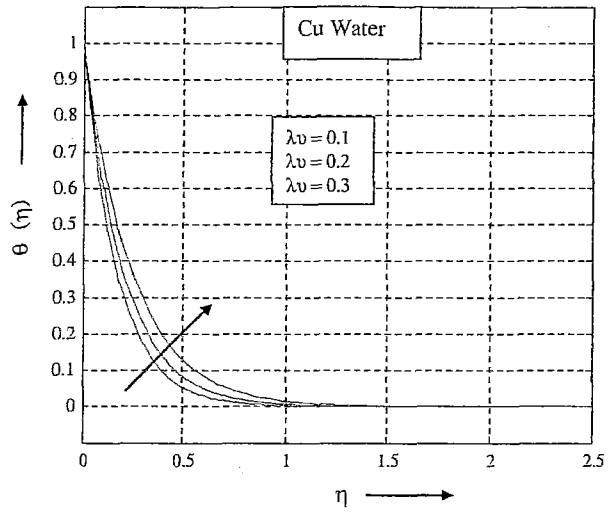

Fig. 8 Temperature profiles for various values of unsteadiness parameter $\zeta = 0.05, N = 0.5, M = 1.0$, $\delta_1 = 1.0$ and $m = 0.0909$ $(\Omega = 30°)$

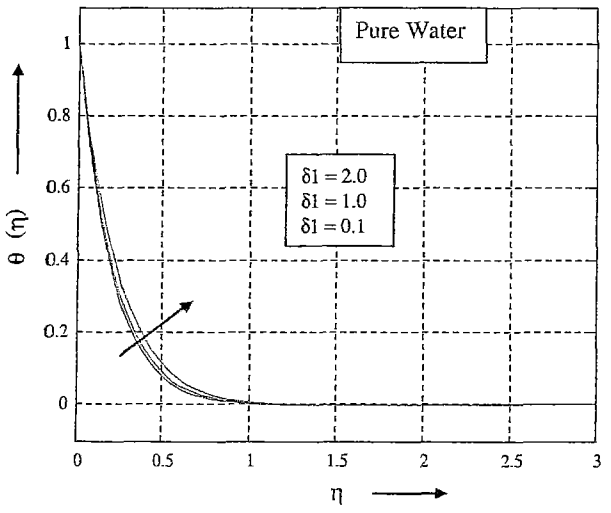

Fig. 9 Effects of heat source over temperature profiles $\zeta = 0.00$, $\lambda_\upsilon = 0.1, N = 0.5$ and $m = 0.0909$ $(\Omega = 30°)$

water) are shown in Figs. 9 and 10. It is observed that the temperature of the base fluid and nanofluid accelerates with increase of heat source parameter. Heat source generates energy which causes the temperature of the fluid to increase in the boundary layer. It is interesting to note that the influence of internal heat generation on temperature distribution is more pronounced on the nanofluid than that of the base fluid. On the other hand, the presence of heat sink in the boundary layer absorbs energy which causes the temperature of the fluid to decrease. All these physical behavior are due to the combined effects of the strength of convective radiation and the size and shape of the nanoparticles in the nanofluid.

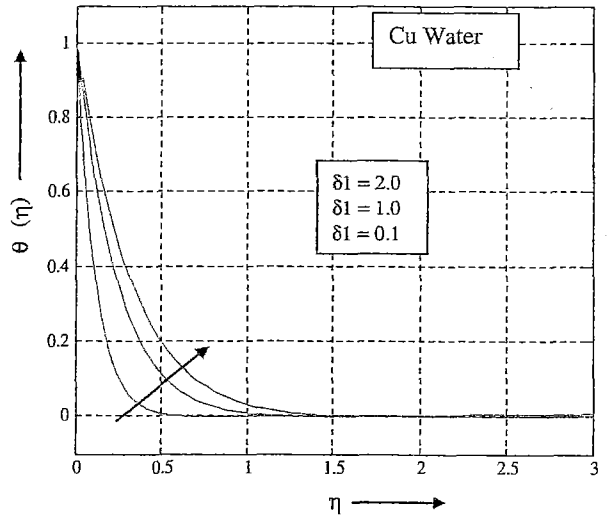

Fig. 10 Effects of heat source over temperature profiles $\zeta = 0.05$, $\lambda_\upsilon = 0.1, N = 0.5$ and $m = 0.0909$ $(\Omega = 30°)$

4 Conclusions

Influence of the copper nanoparticles in the presence of magnetic field on unsteady Hiemenz flow and heat transfer of incompressible Cu-nanofluid along a porous wedge sheet due to solar energy have been analyzed. It is of special interest in this work to consider the similarity transformation is used for unsteady Hiemenz flow. Thermal boundary layer thickness of Cu-nanofluid is stronger than that of the base fluid as the strength of the magnetic field increases because the driving force to the nanofluid decreases as a result of temperature profiles increase. It is noticed that the temperature of a nanofluid is decelerated significantly as compared to that of the base fluid with increase of convective radiation and the internal heat generation on temperature distribution of the nanofluid is more pronounced than that of the base fluid. The thermal conductivity of nanofluid is strongly dependent on the nanoparticle volume fraction. Increase of thermal boundary layer field due to increase in nanoparticle volume fraction and magnetic parameters show that the temperature decreases gradually as we replace Copper, $\zeta = 0.05$ by Silver, $\zeta = 0.1$ and Alumina, $\zeta = 0.15$ in the said sequence. It is seen that the nanofluid decreases whereas the temperature of the nanofluid increases with the increase of unsteadiness parameter. It has been shown that mixing nanoparticles in a liquid (nanofluid) has a dramatic effect on the liquid thermophysical properties such as thermal conductivity. Hiemenz flow over a porous wedge plate plays a very significant role on absorbs the incident solar radiation and transits it to the working fluid by convection. The impact of nanoparticles on the absorption of radiative energy has been of interest for many years for a variety of applications. More recently

Journal : Large 231 | Dispatch : 29-4-2013 | Pages : 9
Article No. : 1163 | LE | TYPESET
MS Code : HMT-12-0378 | CP | DISK

researchers have become interested in the radiative properties of nanoparticles in liquid suspensions especially for medical and other engineering applications. Besides the benefits to the optical and radiative properties, nanofluids provide other benefits such as increased thermal conductivity and particle stability over micron-sized suspensions, which provide potential improvements to the operating efficiency of a direct absorption solar collector. Nanofluids due to solar energy are important because they can be used in numerous applications involving heat transfer and other applications such as in detergency, solar collectors, drying processes, heat exchangers, geothermal and oil recovery, building construction, etc.

References

1. Sharma A, Tyagi VV, Chen CR, Buddhi D (2009) Review on thermal energy storage with phase change materials and applications. Renew Sustain Energy Rev 13:318–345
2. Hunt AJ (1978) Small particle heat exchangers. Lawrence Berkeley Laboratory Report No. LBL-7841, J Renew Sustain Energy
3. Birkoff G (1948) Mathematics for engineers. J Electr Eng 67:1185
4. Yurusoy M, Pakdemirli M (1997) Symmetry reductions of unsteady three-dimensional boundary layers of some non-Newtonian fluids. Int J Eng Sci 35:731–740
5. Yurusoy M, Pakdemirli M, Noyan OF (2001) Lie group analysis of creeping flow of a second grade fluid. Int J Non-Linear Mech 36:955–960
6. Hiemenz K (1911) Die Grenzschicht an einem in den gleichfoÈrmigen FluÈssigkeitsstrom eingetauchten geraden Kreiszylinder. Dingl Poltech J 326:321–410
7. Chamkha AJ, Abdul-Rahim AK (2000) Similarity for hydromagnetic mixed convection heat and mass transfer for Heimenz flow through porous media. Int J Numer Methods Heat Fluid Flow 10:94–115
8. Seddeek MA, Darwish AA, Abdelmeguid MS (2007) Effects of chemical reaction and variable viscosity on hydromagnetic mixed convection heat and mass transfer for Heimenz flow through porous media with radiation. Commun Nonlinear Sci Numer Simul 12:195–213
9. Tsai R, Huang JS (2009) Heat and mass transfer for Soret and Dufour's effects on Heimenz flow through porous medium onto a stretching surface. Int J Heat Mass Transf 52:2399–2406
10. Abdel-Rahman GM (2010) Thermal-diffusion and MHD for Soret and Dufour's effects on Heimenz flow and mass transfer of fluid flow through porous medium onto a stretching surface. Phys B 405:2560–2569
11. Yih KA (1998) The effect of uniform suction/blowing on heat transfer of Magnetohydrodynamic Hiemenz flow through porous media. Acta Mech 130:147–158
12. Kandasamy R, Loganathan P, Puvi Arasu P (2011) Scaling group transformation for MHD boundary- layer flow of a nanofluid past a vertical stretching surface in the presence of suction/injection. Nucl Eng Des 241:2053–2059
13. Vajravelu K, Prasad KV, Lee J, Lee C, Pop I, Van Gorder RA (2011) Convective heat transfer in the flow of viscous Ag–water and Cu–water nanofluids over a stretching surface. Int J Thermal Sci 50:843–851
14. Rana R, Bhargava R (2011) Numerical study of heat transfer enhancement in mixed convection flow along a vertical plate with heat source/sink utilizing nanofluids. Commun Nonlinear Sci Numer Simulat 16:4318–4334
15. Ahmad S, Rohni AM, Pop I (2011) Blasius and Sakiadis problems in nanofluids. Acta Mech 218:195–204
16. Yacob NA, Ishak A, Pop I (2011) Falkner-Skan problem for a static or moving wedge in nanofluids. Int J Thermal Sci 50:133–139
17. Hamad MAA (2011) Analytical solution of natural convection flow of a nanofluid over a linearly stretching sheet in the presence of magnetic field. Int Comm Int J Heat Mass Transfer 38:487–492
18. Magyari E (2011) Comment on the homogeneous nanofluid models applied to convective heat transfer problems. Acta Mech 222:381–385
19. Gill S (1951) A process for the step-by-step integration of differential equations in an automatic digital computing machine. Proc Camb Philos Soc 47:96–108
20. Vafai K, Alkire RL, Tien CL (1985) An experimental investigation of heat transfer in variable porosity media. ASME J Heat Transfer 107:642–647
21. Tien CL, Hong JT (1985) Natural convection in porous media under non-Darcian and non-uniform permeability conditions. In: Kakac S et al (eds) Natural convection. Hemisphere, Washington
22. Fathalah KA, Elsayed MM (1980) Natural convection due to solar radiation over a non absorbing plate with and without heat losses. Int J Heat Fluid Flow 2:41–45
23. Oztop HF, Abu-Nada E (2008) Numerical study of natural convection in partially heated rectangular enclosures filled with nanofluids. Int J Heat Fluid Flow 29:1326–1336
24. Sparrow EM, Cess RD (1978) Radiation heat transfer. Hemisphere, Washington
25. Raptis A (1998) Radiation and free convection flow through a porous medium. Int Comm Heat Mass Transfer 25:289–295
26. Brewster MQ (1972) Thermal radiative transfer properties. Wiley, New York
27. Sattar MA (2011) A local similarity transformation for the unsteady two-dimensional hydrodynamic boundary layer equations of a flow past a wedge. Int J Appl Math Mech 7:15–28
28. Aminossadati SM, Ghasemi B (2009) Natural convection cooling of a localized heat source at the bottom of a nanofluid-filled enclosure. Eur J Mech B Fluids 28:630–640
29. Maxwell JC (1891) A treatise on electricity and magnetism 2 unabridged, 3rd edn. Clarendon Press Oxford, UK
30. Kafoussias NG, Nanousis ND (1997) Magnetohydrodynamic laminar boundary layer flow over a wedge with suction or injection. Can J Phys 75:733
31. Schlichting H (1979) Boundary layer theory. McGraw Hill Inc, New York
32. White FM (2006) Viscous fluid flows, 3rd edn. McGraw-Hill, New York

Journal : Large 231 | Dispatch : 29-4-2013 | Pages : 9
Article No. : 1163 | LE | TYPESET
MS Code : HMT-12-0378 | CP | DISK